Journal of Alloys and Compounds 509 (2011) 8165–8170

Contents lists available at ScienceDirect

Journal of Alloys and Compounds

journal homepage: www.elsevier.com/locate/jallcom

Internal friction, dilatometric and calorimetric study of anelasticity in Fe–13 at.% Ga and Fe–8 at.% Al–3 at.% Ga alloys

I.S. Golovin[a,*], Z. Belamri[b], D. Hamana[b]

[a] Departments of Physical Materials Science and Physical Metallurgy of Non-Ferrous Metals, National Research Technological University "MISiS", Leninskij ave. 4, 119049 Moscow, Russia

[b] Phases Transformation Laboratory, Mentouri University of Constantine, Ain El Bey Road, 25000 Constantine, Algeria

ARTICLE INFO

Article history:
Received 24 April 2011
Received in revised form 27 April 2011
Accepted 28 April 2011
Available online 24 May 2011

Keywords:
Multiphase intermetallics
Internal friction
Dilatometry
DSC
Defects: point defects
Vacancies
Grain boundaries
Ordering process

ABSTRACT

This paper investigates the structural transitions associated with different cooling rates from a high temperature disordered state and the effect of substitution of Ga atoms by Al atoms in Fe–Ga binary alloys on the ordering processes. Two iron-based low carbon (about 0.04 at.% C) alloys Fe–13 at.% Ga and Fe–8 at.% Al–3 at.% Ga are studied. Internal friction, dilatometric and calorimetric tests are carried out to check ordering in these alloys and contribution of structural defects to relaxation spectrum. Several thermally activated internal friction peaks have been observed and their activation parameters evaluated by means of temperature and frequency dependent internal friction tests using forced vibration. For most of these peaks physical mechanisms are proposed. Apart from these thermally activated relaxation peaks, a structural, frequency independent relaxation takes place at 250–300 °C. Dilatometric and DSC curves show the appearance of a contraction effect in the same temperature range. This effect was studied in alloys cooled down with different cooling rates. We believe that the frequency independent internal friction peak (denoted as the P3 peak in this paper) and peaks at dilatometric and DSC curves are controlled by the same structural mechanism and therefore the activation energy for this anelastic mechanism is derived from DSC data.

1. Introduction

The Fe–Ga alloys, 'Galfenol', have low ductility [1] caused by ordering of Ga atoms in bcc iron (B2, $D0_3$, $D0_{19}$ and $L1_2$), where the type of order depends on temperature and concentration of Ga atoms in iron [2,3]. Fe–Ga alloys with Ga < 20 at.% are also known by their high damping capacity [4] due to high values of magnetostriction [5], which are typical for soft-magnetic materials with positive anisotropy energy [6]. In contrast to other bcc alloys with tendency to ordering, very little information can be found in literature on amplitude independent mechanisms of internal friction in Fe–Ga alloys [4,7,8].

Several internal friction effects caused by thermally activated phenomena have been discovered in paper [9]: the Snoek-type relaxation, composed of the P1 and P2 peaks due to carbon atom jumps in the Fe–C–Fe and Fe–C–Ga surrounding (total peak is denoted as the $P_{1/2}$ peak), the Zener relaxations due to reorientation of Ga–Ga atom pairs denoted as the P4 peak, and the grain boundary relaxation – the P5 peak. At the same time, authors [9] have reported two anelastic effects denoted as the P3 and P4 peaks in the temperature range from 150 to 300 °C the origin of which were not well explained. These two anelastic effects were even not well reproducible because their magnitude and temperature depend on specimen heat treatment and test conditions. It was suggested that these effects might be caused by a structural transformation in the Fe–13 at.% Ga alloy.

Both Fe–Al and Fe–Ga alloys exhibit high values of amplitude dependent damping, which is higher in the Fe–Ga alloy due to higher values of magnetostriction [4]. Unfortunately, in contrast with cheap and ductile Fe–Al high damping alloys the Fe–Ga alloys are expensive and rather brittle. Thus the idea to develop a ternary high damping Fe–Al–Ga alloy looks very attractive. Our interest in this ternary alloys is not limited by study of amplitude dependent damping (to be reported elsewhere) but we also want to study temperature dependent damping in ternary Fe–Al–Ga alloys the chemical composition of which is based on the idea of substituting Al atoms by Ga atoms in well known high damping Fe–11 at.% Al alloys [10]. The main purpose of this paper is the study of structural mechanisms which lead to temperature and frequency dependent internal friction effects. It will also contribute to better understanding similar effects in Fe–Al [11], Fe–Ge [12] and more complex alloyed systems like Fe–Si–Al [13] or Fe–Al–Cr [14].

* Corresponding author.
E-mail address: i.golovin@tu-bs.de (I.S. Golovin).

0925-8388/$ – see front matter © 2011 Elsevier B.V. All rights reserved.
doi:10.1016/j.jallcom.2011.04.138

2. Experimental methods

Fe–Ga and Fe–Al–Ga alloys of nominal compositions 13 at.% Ga and 8 at.% Al + 3 at.% Ga were prepared by induction melting. High purity raw materials (Fe: 99.99%, Ga: 99.999%, Al: 99.999%, C: 99.9999%) have been used for the production. A small amount of carbon (~0.01 wt.%) was added to the alloy in order to check the appearance of the Snoek peak reported in paper [9]. The carbon powder was embedded into Fe-foil to avoid fogging during melting. The actual concentration of Ga in Fe–Ga alloy was determined by electron-probe microanalysis to be 13.6 at.%. Specimens were annealed at 1000 °C for 24 h in vacuum to homogenize the structure and then cooled in air inside quartz ampoules.

The internal friction (IF), i.e. damping Q^{-1} ($Q^{-1} \cong \tan\varphi$, where φ is the phase lag between the applied cyclic stress and the resulting strain) was measured as a function of temperature at commercial dynamical mechanical analyser DMA Q800 TA Instruments between −130 and 570 °C using forced bending vibrations of 60 mm × 4 mm × 1 mm specimens in the range between 0.05 and 50 Hz with $\varepsilon_0 = 5 \times 10^{-5}$ and heating rate of 1 K/min.

The dilatometric analysis was carried out under argon using a DI24 Adamel Lhomargy dilatometer connected to a microcomputer with software (Logidil) to analyse obtained results. The DSC measurements were carried out under argon with a Setaram DSC 131. Cylindrical samples of 5 mm in diameter and 2 mm long were used for DSC analysis and cylindrical samples of 5 mm in diameter and 20 mm long were used for dilatometric analysis. The thermal cycle applied consisted of heating from room temperature to 800 °C for dilatometer and to 690 °C for DSC.

3. Results and discussion

3.1. Internal friction tests

The Fe–13 at.% Ga and Fe–8 at.% Al–3 at.% Ga alloys have relatively high internal friction background at room and elevated temperatures (Fig. 1(a) and (b)). The main source of background damping is magneto-mechanical damping. This can be easily proved by applying axial magnetic field which drastically, in order of magnitude, decreases the damping level (data are not included in this paper). Example of amplitude dependent internal friction curve is given in inset to Fig. 1(a). The maximum of this curve corresponds to maximum of magneto-mechanical damping at room temperature. Absolute values of Young's modulus in our tests (Figs. 1 and 2) are not precise because of the deviations of the specimen's shape from a rectangular bar. Nevertheless, they are still in a reasonable agreement with values given in paper [15]. Modulus dependence in Fe–13 at.% Ga alloy has clear inverse effect in the temperature range from 250 to 350 °C for air cooled specimen and from 200 to 270 °C for water quenched specimen. Results for Fe–8 at.% Al–3 at.% Ga alloy (Fig. 1(b)) are similar to Fe–13 at.% Ga: the same peaks can be distinguished. The difference between two alloys is a smaller effect of reverse modulus behaviour and lower high temperature background, which results in better resolution of the high temperature IF peak in ternary alloy with lower content of alloying elements.

Fig. 1 shows the temperature dependent internal friction curves, TDIF, for both alloys as measured at forced bending vibrations using DMA Q800 setup; the samples have been cooled from homogenising temperature 1000 °C in air inside air-free quartz ampoule. The low-temperature P_{LT} peak position, earlier observed in Fe–Ge and Fe–Al alloys [9,11,16], depends on frequency. We suppose that this peak corresponds to Hasiguti-type relaxation [7] of dislocations with neighboring self lattice defects. Complex Snoek relaxation in a ternary alloy (e.g., Fe–C–Me, where Me is metal) system contains several elementary relaxation processes. The $P_{1/2}$ peak, also observed earlier in Fe–Al, Fe–Co, Fe–Ge and Fe–Si alloys [8], is a complex Snoek-type peak: it appears due to carbon atom jumps in bcc solid solution near both Fe atoms (the P1 peak corresponds to carbon jumps in positions Fe–C–Fe) and Ga atoms (the P2 peak corresponds to carbon jumps in positions Fe–C–Ga or Fe–C–Al). The P1 and P2 peak locations are relatively close to each other and they produce one not symmetrical peak denoted in this paper as the $P_{1/2}$ peak. The occurrence of the P2 peak, sometimes called i–s (interstitial–substitution) peak, is typical for several Fe–C–Me alloys with substitutional not strong carbide forming Me atoms and

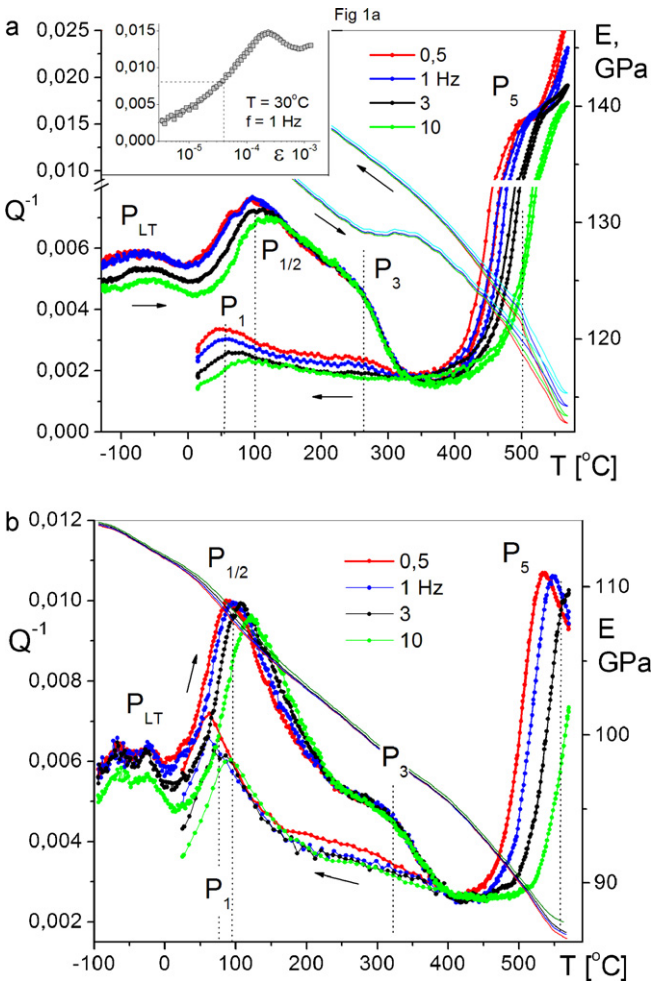

Fig. 1. Temperature dependent internal friction, Q^{-1}, and elastic modulus, E, in air cooled Fe–13 Ga (upper) and Fe–8 Al–3 Ga (lower) figures. Heating rate 1 K/min, cooling rate 3 K/min, frequencies used: 0.5, 1, 3, 10 Hz, maximal amplitude of deformation $\varepsilon_0 = 5 \times 10^{-5}$. Inset to Fig. 1a shows amplitude dependent internal friction at 1 Hz and 30 °C.

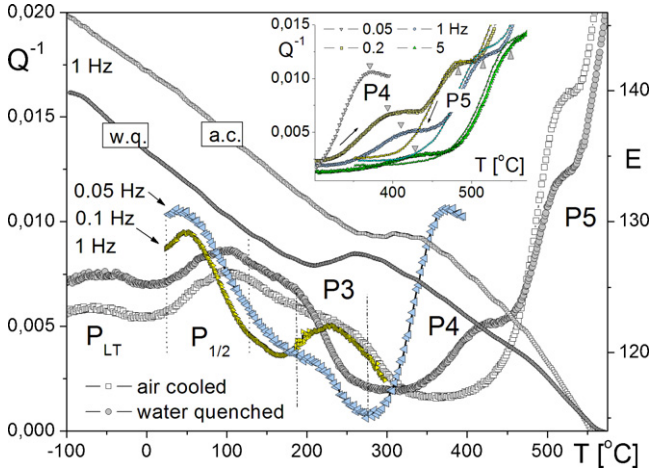

Fig. 2. Temperature dependent internal friction, Q^{-1}, and elastic modulus, E, in air cooled from 1000 °C and additionally water quenched from 800 °C Fe–13 Ga specimen for measuring frequency 1 Hz, heating rate 1 K/min, and maximal amplitude of deformation $\varepsilon_0 = 5 \times 10^{-5}$. Additional curves for air cooled specimen measured at 0.1 Hz and water quenched specimen measured at 0.05 Hz are added in the temperature range from 20 to 300 °C and 20–400 °C correspondingly. Inset: TDIF curves in the vicinity of P4 and P5 peaks as measured at different frequencies at heating and cooling.

Table 1
Activation parameters of the peaks studied (see Fig. 1).

$P_{1/2}$ peak		P_1 peak		P4 peak		P5 peak		P3 peak
Complex Snoek peak		Snoek peak		Zener peak		GB peak		DSC results
H, eV	τ_0, s	H, eV	τ_0, s	H, eV	τ_0, s	H, eV	τ_0, s	H, eV
heating		cooling		heating				
Fe–13 at.% Ga–C								
1.1	2×10^{-16}	0.88	8×10^{-15}	2.2	10^{-17}	2.7	10^{-18}	0.93
Fe–8 at.% Al–3 at.% Ga–C								
1.07	4×10^{-16}	0.8	5×10^{-14}	not studied		2.8	10^{-18}	0.97

for Nb–Ti–O alloys [17]. Taking the atomic (Goldschmidt) radii for Fe, Ga and Al as 128, 135 and 143 pm, correspondingly, the relative distortion of crystalline lattice around substitute atom ($\Delta r/r_{Fe}$) is Ga/Fe = 5.5% and Al/Fe = 11.2%. This elastic distortion around the solute atom due to its size misfit plays a decisive role in the change of activation energy of carbon atom jump and in the P2 peak formation.

The P3 and P4 peaks are discussed below. At cooling from 570 °C the P3 and P4 peaks practically disappear. The same happens to the P2 peak component of the complex Snoek-type peak, while the P1 component of the $P_{1/2}$ peak is present in TDIF curves. The P_{LT} peak also disappears from TDIF curves after specimen annealing (these data are not presented in Fig. 1).

The P4 peak appears in the TDIF spectra only in the case of water quenching of the Fe–13 Ga specimen (Fig. 2, curves are given for 1 Hz only) at heating. At cooling the P4 peak disappears. Inset to Fig. 2 shows clear temperature dependence of the P4 and P5 peaks position on measuring frequency. We believe that the P4 peak appears due to Zener relaxation and is caused by reorientation of substitute atom pairs (Ga–Ga) in substitutional solid disordered solution, and the P5 peak is the grain boundary peak. The P4 peak is suppressed if structure is ordered, i.e. after annealing, but it is well observed in the quenched state. We have not observed the P4 peak in the Fe–8 at.% Al–3 at.% Ga alloy which may be the consequence of lower amount of alloying elements in this alloy. The P3 peak observed in both alloys is frequency independent according to our experiments in used frequency range of forced vibrations. In the quenched-in state the peak is observed at lower temperatures as compared to air cooled specimen.

In contrast with the P3 peak, the position of the P_{LT}, $P_{1/2}$, P4 and P5 peaks depends on the measuring frequency. Thus, these peaks are thermally activated peaks, and their temperature rises with the measurement frequency according to the condition $\omega \times \tau = 1$ for a frequency dependent Debye peak of internal friction represented by:

$$Q^{-1} = \Delta \frac{\omega\tau}{(1 + (\omega\tau)^2)}, \quad (1)$$

where τ is the relaxation time and Δ is the relaxation strength. The relaxation time is controlled by thermally activated atomic jumps,

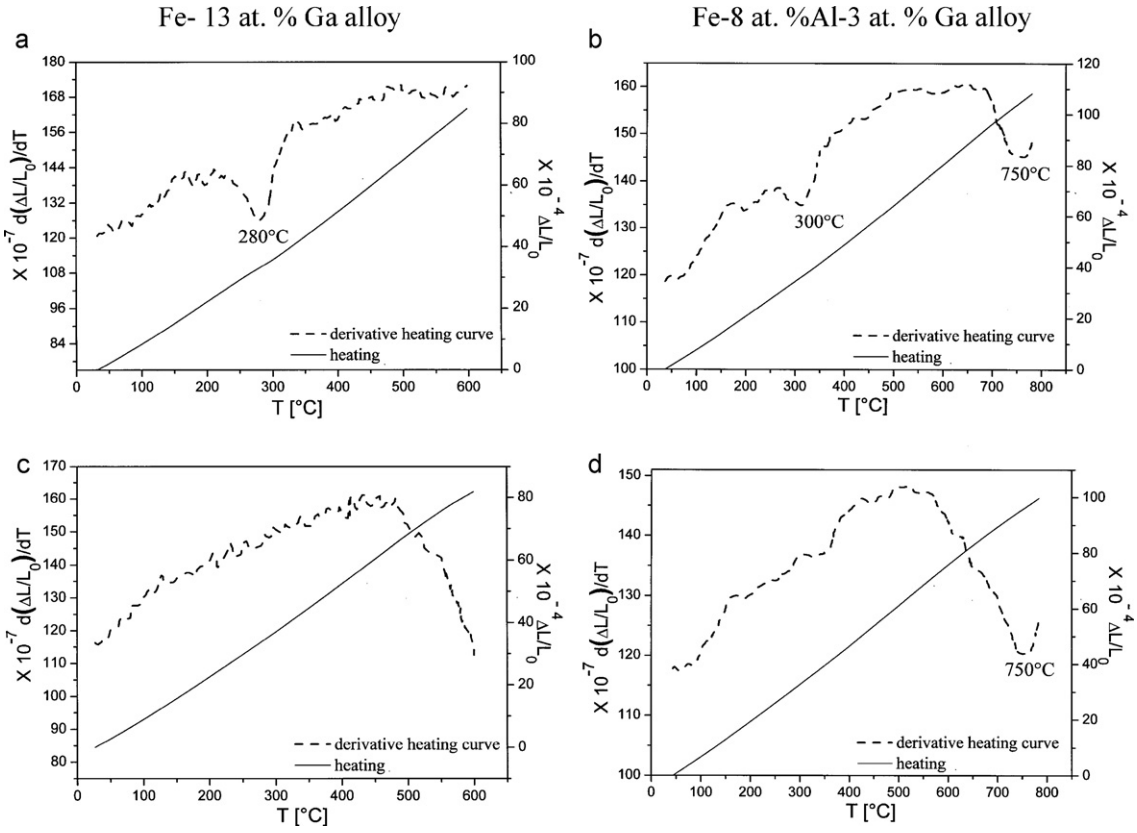

Fig. 3. Dilatometric curves and derivative heating curves of homogenised and water quenched (a and b), homogenised and air cooled (c and d) Fe–13 at.% Ga and Fe–8 at.% Al–3 at.% Ga alloys (heating rate10 K/min).

so that its temperature dependence is described by an Arrhenius equation:

$$\tau^{-1} = \tau_0^{-1} \times \exp\left(\frac{-H}{k_B T}\right), \quad (2)$$

where H is the activation energy, τ_0 is the pre-exponential factor in the relaxation time and k_B is the Boltzmann factor. Values of H (accuracy ±0.05 eV) and τ_0 for the $P_{1/2}$, P4 and P5 peaks at heating and P1 peak at cooling are calculated by Arrhenius shift and collected in Table 1.

Activation parameters of the peaks included in the table are rather similar for both alloys, at least within the accuracy of our experiments. In contrast to these peaks, the P3 peak temperature does not depend on the frequency used in experiments, see Figs. 1 and 2, and is accompanied by inverse modulus behaviour. Its activation energy included in the table is evaluated from DSC tests discussed below. The temperature of this inverse modulus behaviour decreases if we use the quenched specimen instead of the annealed one. Such modulus behaviour may take place in case of recrystallisation (known as Köster effect, e.g. recently reported in [18]), decrease in vacancy concentration or ordering, and ferro- to paramagnetic transition [7]. Similar inverse modulus effect at around 300 °C in Fe–17 at.% Ga alloy was explained by ferro- to paramagnetic transition in paper [4]. In Fe–13 at.% Ga with the Curie point at around 720 °C, this second order transition cannot be the reason for the inverse modulus effect. The P3 peak takes place at the beginning of this modulus increase: the P3 and P1/2 peaks are better separated if low frequencies are used (Fig. 2, curves for 0.1 and 0.05 Hz) and are merged at higher frequencies.

According to the existing diagrams, the temperature range of inverse modulus behaviour corresponds to disorder–order ($D0_3$) transition. The $D0_3$ order was found in Fe–14 at.% Ga composition: quenching suppresses $D0_3$ formation, whereas slow-cooling favors it [19,20]. Thus, slow-cooling or heating may stabilize the $D0_3$–A2 two-phase field to Ga contents also in the range of $x \leq 14$. Precipitation of the $D0_3$ clusters constrained within the A2 matrix is well known in the compositionally similar Fe–Al alloys as the K-state [3], and is supposed to take place in Fe–Ga alloys [21]. Ordering leads to decrease in magneto-mechanical damping. In case of heat treatment at low temperatures, e.g. after heating to 400 °C, the Young's modulus plateau and the P3 peak vanish, making the total IF peak between 75 and 250 °C narrower.

3.2. Dilatometric and DSC tests

Dilatometric and DSC tests were carried out to check if ordering in the studied alloys may take place or not. Dilatometric curve with heating rate 10 K/min of 2 h homogenised at 800 °C and water quenched Fe–13 at.% Ga alloy is presented in Fig. 3(a). Indeed, the derivative of this dilatometric curve shows a contraction toward 280 °C (for heating rate 10 K/min) or 260 °C (for heating rate 1 K/min) (Fig. 4(a)). The same effects are detected on the dilatometric curve of specimen homogenised for 2 h at 730 °C and then water quenched. This temperature is close to the temperature of the P3 internal friction peak in a quenched state, if the difference in heating rate is considered.

On the dilatometric and derivative heating curve of the 2 h homogenised at 800 °C and then slowly cooled sample, the contraction disappears (Fig. 3(c)). The $D0_3$ ordered domains are formed during the slow cooling.

For the Fe–8 at.% Al–3 at.% Ga alloy the contraction is observed at 300 °C and 230 °C with heating rate 10 K/min or 1 K/min, respectively (Fig. 4(b)); it is explained by the same effect – formation of $D0_3$ ordered phase. One can observe a contraction toward 750 °C on dilatometric curves of the Fe–8 at.% Al–3 at.% Ga alloy after water quenching Fig. 3(b) or air cooling Fig. 3(d) due to the magnetic transition (Curie point).

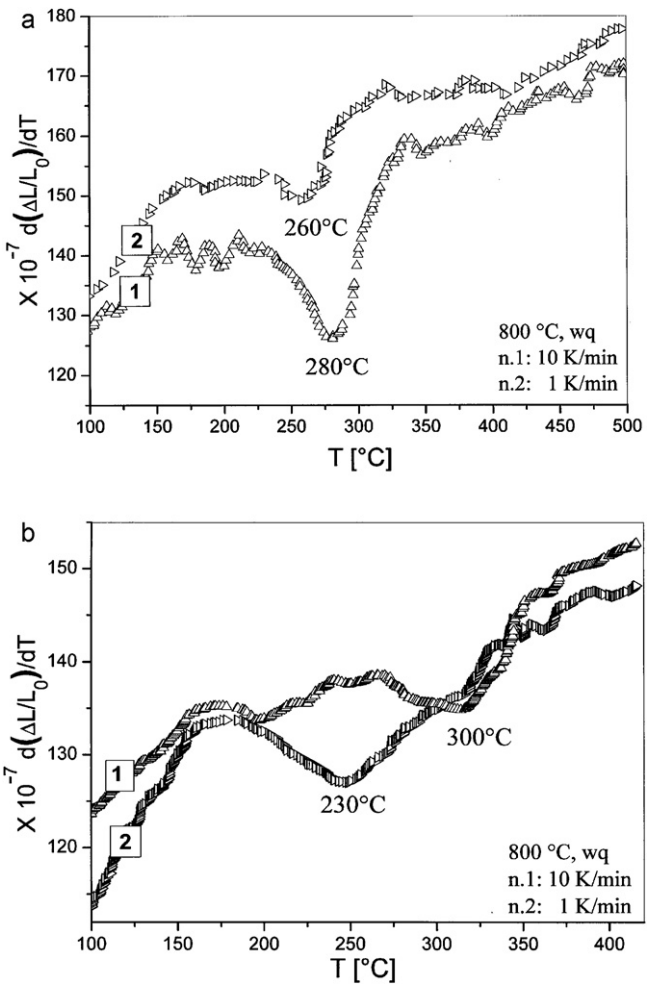

Fig. 4. Derivative heating curves of homogenised and water quenched samples: (a) Fe–13 at.% Ga alloy: (1) heating rate 10 K/min and (2) heating rate 1 K/min; (b) Fe–8 at.% Al–3 at.% Ga alloy: (1) heating rate 10 K/min and (2) heating rate 1 K/min.

The DSC obtained with heating rate 10 K/min curves for homogenised 2 h at 800 C and water quenched samples (Fig. 5(a) and (b)) show an exothermic effect toward 288 °C (for Fe–13 at.% Ga alloy) and 304 °C (for Fe–8 at.% Al–3 at.% Ga alloy) which is caused by the same effect – formation of the $D0_3$ ordered domains. The same effect is obtained at heating rates of 15, 20 and 30 °C/min with a shift of the peak toward a higher temperature.

The comparison of the IF, DSC and dilatometric curves confirms the results obtained in [19]: quenching suppresses $D0_3$ formation, whereas slow-cooling favors it. Thus, at slow heating rate (1 K/min) an internal friction peak takes place due to ordering. Very slow cooling stabilizes the $D0_3$ domains for the concentration of Ga even below 14%, which is shown on the obtained dilatometric curves for furnace or air cooled specimen, by the disappearance of the observed contraction on the dilatometric curve of the water quenched specimen at 730 °C and 800 °C. The contraction observed on the dilatometric curves for water quenched specimens both at 730 °C and 800 °C, confirms the results obtained by internal friction method by the shift of P3 peak to lower temperatures and the Young's modulus behaviour in the temperature range of 225–300 °C, which is linked to the ordering process.

To estimate the activation energy of the exothermic peak in this range, i.e. the activation energy of formation of the ordered $D0_3$ phase in Fe–13 at.% Ga and Fe–8 at.% Al–3 at.% Ga alloys, Starink's

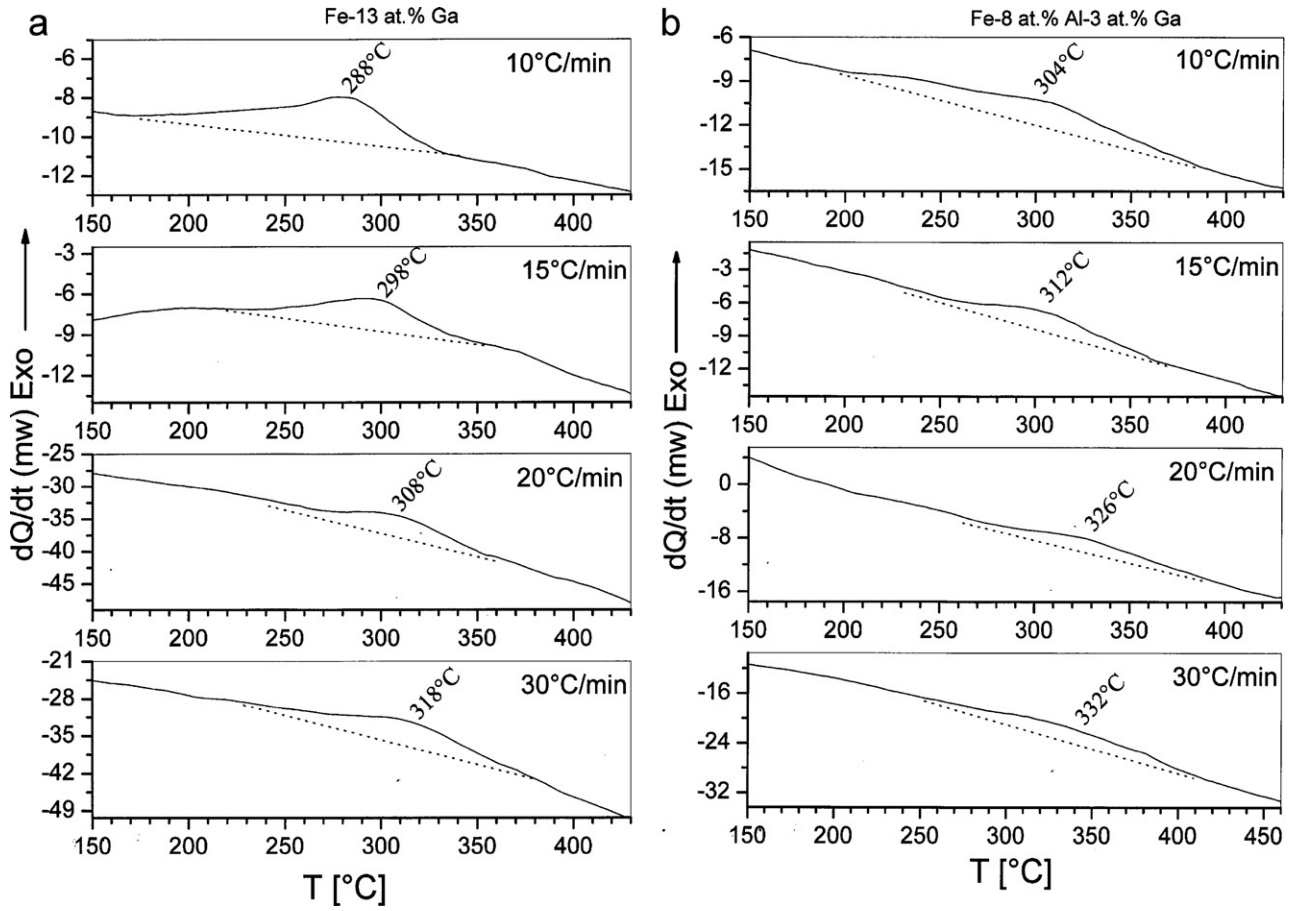

Fig. 5. DSC curves in the range of $D0_3$ ordered phase formation in Fe–13 at.% Ga (a) and Fe–8 at.% Al–3 at.% Ga (b) alloys heated 2 h at 800 °C, water quenched then heated with different rates.

[22], Kissinger's [23] and Ozawa's [24] methods (see Eqs. (3)–(5), correspondingly) and results presented in Fig. 5 were used:

$$-\ln\frac{\beta}{T_m^{1.92}} = -1.0008\frac{H_{act}}{RT_m} + C_1 \quad (3)$$

$$\ln\frac{\beta}{T_m^2} = -\frac{H_{act}}{RT_m} + C_2 \quad (4)$$

$$\ln\beta = -1.0516\frac{H_{act}}{RT_m} + C_3 \quad (5)$$

where β, T_m and R represent the heating rate, the peak temperature and the gas constant, respectively. The three methods give similar values of the activation energy for each studied alloy. The activation energy H_{act} deduced by Starink's method from the right-hand side $\ln(T_p^{1.92}/\beta)$ as function of $(1000/T_m)$ is represented in Fig. 6. The calculated value of activation energy of $D0_3$ ordering process, which controls the P3 internal friction peak according to obtained data, equals to 0.93 eV for Fe–13 at.% Ga alloy and 0.97 eV for Fe–8 at.% Al–3 at.% Ga alloy. Thus, activation energy of ordering in the binary alloy is a little lower than that obtained for the ternary alloy, which means that the ordering process in Fe–8 at.% Al–3 at.% Ga requires

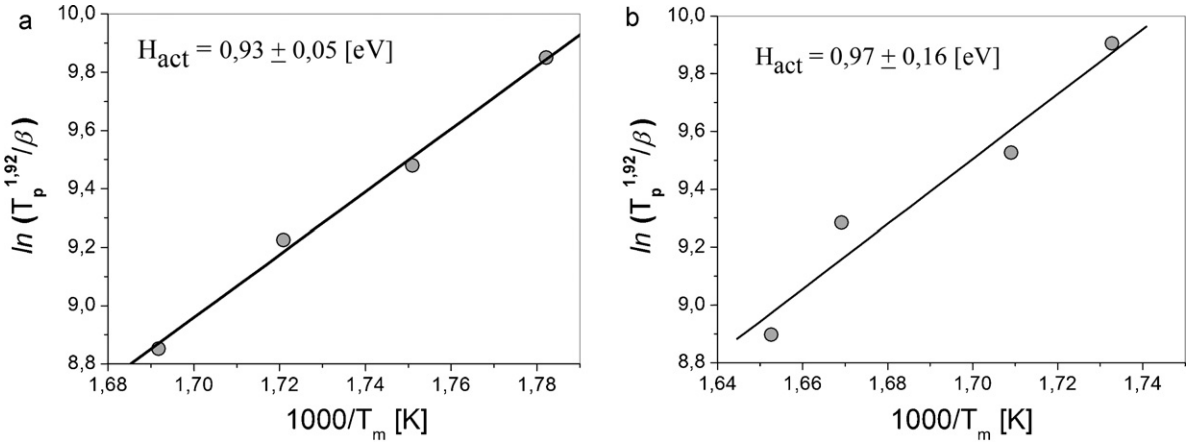

Fig. 6. Starink's plots to obtain the activation energy H_{act} of $D0_3$ ordered phase in Fe–13 at.% Ga (a) and Fe–8 at.% Al–3 at.% Ga (b) alloys.

more energy. We suppose that it is the ordering process which controls the P3 internal friction peak and values of activation energy for ordering process derived from DSC data correspond also to the P3 peak (Table 1).

4. Conclusion

The use of different experimental techniques (internal friction, dilatometry and DSC) to study phase transitions in Fe–13 at.% Ga and Fe–8 at.% Al–3 at.% Ga alloys shows that the appearance of an effect on the obtained curves in the temperature range of 250–300 °C is due to ordering processes in studied alloys. Several thermally activated internal friction peaks were identified by their activation parameters as the Snoek-type, Zener and grain boundary relaxation.

Acknowledgement

This study is partly supported by RFFI grant 11-08-01113.

References

[1] J. Li, X. Gao, J. Zhu, J. Li, M. Zhang, JALCOM 484 (2009) 203–206.
[2] O. Kubaschewski, Iron-Binary Phase Diagrams, Springer-Verlag, Berlin, 1982.
[3] T.B. Massalski, Binary Alloy Phase Diagrams, 2nd ed., ASM, OH, 1990, p. 1740.
[4] M. Ishimoto, H. Numakura, M. Wuttig, Materials Science and Engineering A 442 (2006) 195–198.
[5] M. Huang, Y. Du, R.J. McQueeney, T.A. Lograsso, Journal of Applied Physics 107 (2010) 053520.
[6] C. Mudivarthi, S.-M. Na, R. Schaefer, M. Laver, M. Wttig, A.B. Flatau, Journal of Magnetism and Magnetic Materials 322 (2010) 2023–2026.
[7] M.S. Blanter, I.S. Golovin, H. Neuhäuser, H.-R. Sinning, Internal Friction in Metallic Materials: A Handbook, Springer, 2007.
[8] I.S. Golovin, in: Y.N. Berdovsky (Ed.), Intermetallics Research Trends, Nova Science Publishers Inc., 2008, pp. 65–133.
[9] I.S. Golovin, A. Rivière, Intermetallics 19 (2011) 453–459.
[10] V.A. Udovenko, S.I. Tishaev, I.B. Chudakov, Physics Doklady 38 (4) (1993) 168–170 (in English) (Dokladi akademii nauk 329 (5) (1993) 585–588 (in Russian)).
[11] I.S. Golovin, S.V. Divinski, J. Čížek, I. Procházka, F. Stein, Acta Materialia 53 (2005) 2581–2594.
[12] I.S. Golovin, H. Neuhäuser, H.-R. Sinning, C. Siemers, Intermetallics 18 (2010) 913–921.
[13] H.-R. Sinning, I.S. Golovin, A. Strahl, O.A. Sokolova, T. Sazonova, Materials Science and Engineering A 521–522 (2009) 63–66.
[14] I.S. Golovin, A. Rivière, Materials Science and Engineering A 521–522 (2009) 67–72.
[15] K. Chen, L.M. Cheng, Physica Status Solidi B 244 (10) (2007) 3583–3592.
[16] A. Strahl, S.B. Golovina, I.S. Golovin, H. Neuhäuser, Journal of Alloys and Compounds 378 (2004) 268–273.
[17] L. Yu, F. Yin, D. Ping, Physical Review B 75 (2007) 174105.
[18] I.S. Golovin, Physics of Metals and Metallography 110 (4) (2010) 405–413.
[19] H. Cao, F. Bai, J. Li, D.D. Viehland, T.A. Lograsso, P.M. Gehring, Journal of Alloys and Compounds 465 (2008) 244–249.
[20] J. Liu, F. Yi, C. Jiang, Journal of Alloys and Compounds 481 (2009) 57–59.
[21] A.G. Khachaturyan, D. Viehland, Metallurgical and Materials Transactions A: Physical Metallurgy and Materials Science 38A (2007) 2308–2316.
[22] M.J. Starink, Thermochimica Acta 404 (2003) 163–176.
[23] H.E. Kissinger, Analytical Chemistry 29 (1957) 1702–1706.
[24] T. Ozawa, Journal of Thermal Analysis 2 (1970) 301–324.